Supplementary Information (SI) for New Journal of Chemistry.
This journal is © The Royal Society of Chemistry and the Centre National de la Recherche Scientifique 2025

Supplementary material

The reagents and sources, instruments, and characterization methods involved in the paper will all be presented in the supporting materials. In addition, we present some of the chart data here.

Materials and reagents

Vanillin ($C_8H_8O_3$, 99.8%) was provided by Tianjin Guangfu Fine Chemical Research Institute, China. Vanillyl alcohol ($C_8H_{10}O_3$, 99.7%) was provided by TCI Chemical Industry Development Co., Ltd., China. N-decane ($C_{10}H_{22}$, 99.7%) was provided by Tianjin Kemiou Chemical Reagent Co., Ltd., China. Boric acid (H_3BO_3, 99.8%) and isopropanol (C_3H_8O, 99.8%) were provided by Shanghai Aladdin Biochemical Technology Co., Ltd., China. Melamine ($C_3H_6N_6$, 99.8%) and 2-benzimidazole thiol ($C_7H_6N_2S$, 99.8%) were provided by Shanghai Macklin Biochemical Technology Co., Ltd., China. All the chemicals were used directly without any further treatment.

Catalyst characterization

To obtain the microstructure of the catalyst, a transmission electron microscope (TEM, model: Thermo Fisher Scientific Talos F200X, accelerating voltage: 200 kV) with energy-dispersive X-ray mapping (EDX) of the catalyst was carried out. The phase structure analysis of catalyst samples was carried out by powder X-ray diffraction (XRD, model: 300-2000PS2). Raman spectroscopy (Raman, model: Renishaw inVia Reflex, excitation wavelength λ = 532 nm) was used to analyze and identify the structure of the catalyst, including the degree of defects and the degree of graphitization. X-ray photoelectron spectroscopy (XPS, model: ESCALAB 250Xi, the excitation source was Al Kα ray) was used to determine the type, chemical valence, and relative abundance of the elements on the catalyst sample surface. Fourier transform infrared spectroscopy (FTIR, model: Bruker TENSOR 27, resolution 0.5 cm^{-1}, wavelength

range 500-4000 cm^{-1}) was used to examine and determine the functional groups on the catalyst surface. The type of acid sites of the catalysts was determined by pyridine infrared analysis (Py-IR, model: NEXUS 5700 type, CO_2 carrier gas flow of 30 mL/min). The basicity and alkalinity of the catalyst were determined by CO_2 temperature-programmed desorption (CO_2-TPD, model: PCA-1200, 30 mL/min CO_2 carrier gas flow). The acidity and acid content of the catalyst were analyzed and determined by NH_3 temperature-programmed desorption (NH_3-TPD, model: PCA-1200, 30 mL/min NH_3 carrier gas flow).

Due to the restriction of site influence region and N-B site unit cell region, the flat adsorption configuration was found unstable and even destroyed by global optimization search of structural relaxation. Therefore, the vertical adsorption configuration of aldehyde was selected as the adsorption model for subsequent studies. After a series of optimized structural relaxation, it is easy to find that the aldehyde group on VAN is mainly adsorbed on the active group of N-B site, and the O on the aldehyde group is mainly adsorbed on the B atom of N-B site, forming a relatively stable adsorption configuration. After adsorption of VAN molecule, the geometric structure and electronic density of the aldehyde group adsorbed on VAN at different N-B sites will change obviously, which is mainly due to the N-B coordination The negative charge density of the B atom is relatively absent, which has been demonstrated in Bader's charge calculations.

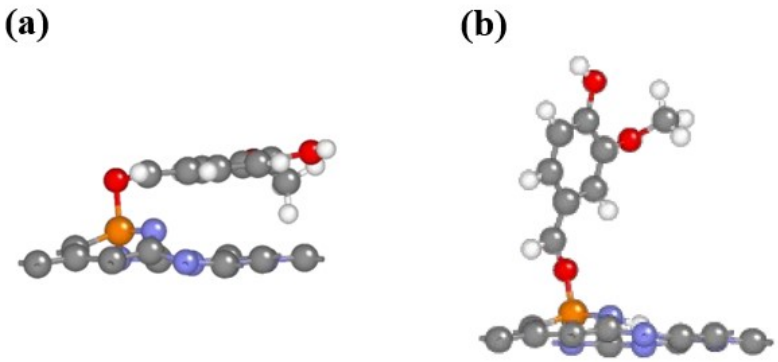

Figure S1. (a) lying adsorption configuration and (b) vertical adsorption configuration of VAN molecule at N-B site

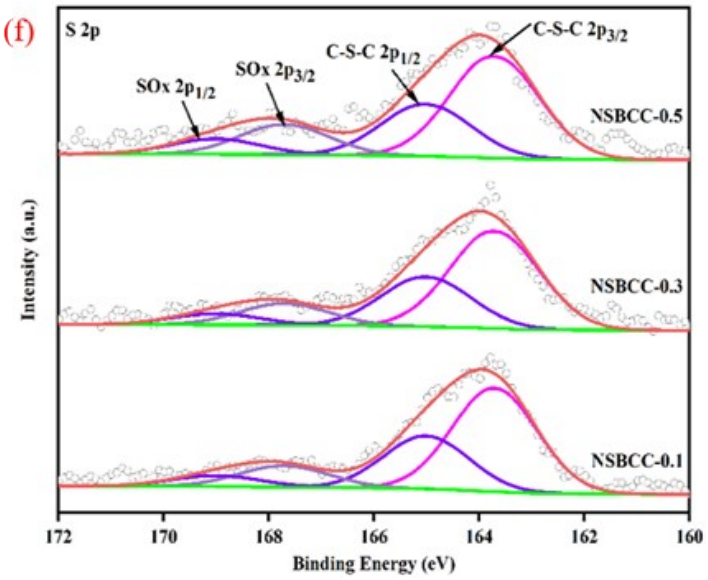

Figure S2. The high-resolution XPS spectra for S 2p

Table S1 Research progress on VAN to MMP

Catalyst	Conversion (%)	Selectivity (%)	Ref.
200-Pt/Mo_2TiC_2	100	VA (96)	1
Pd/RPR	100	96.8	2
Pd/MS-HZSM-5(30)	99	94.7	3
Pd/PHS	>99	98.2	4
$Pd_1/WO_{2.72}$	99	99	5
PdNi/CuFeO	99.40	99.20	6
Pd@MOF	99	99	7
CoMo/BC	99.24	92.79	8
Ni_xCu_y/BC	100	88	9
Co@C	100	90	10
Ni/MP (M=Ti, Zr, Nb, La, Ce)	97.25	88.39	11
Co@NPC-KLB	100	88.49	12
Ni-MMT	>99	95.20	13

References

1. Z. Zhao, S. Huang, G. Dong, Y. Chen, M. Wang, M. Xia, X. Song, X. Li, Z. Wei and J. Wang, *Chemical Engineering Science*, 2024, DOI: 10.1016/j.ces.2024.120616.
2. M. Qiao, J. Ran, T. Yang, Z. Liu and K. Yao, *Catalysis Today*, 2024, DOI: 10.1016/j.cattod.2024.114778.
3. J. Ran, L. Alfilfil, J. Li, R. Yangcheng, Z. Liu, Q. Wang, Y. Cui, T. Cao, M. Qiao, K. Yao, D. Zhang and J. Wang, *ChemCatChem*, 2022, DOI: 10.1002/cctc.202200397.
4. R. Yangcheng, Y. Cui, S. Luo, J. Ran and J. Wang, *Microporous and Mesoporous Materials*, 2023, DOI: 10.1016/j.micromeso.2023.112460.
5. L. Zhijun, L. Xiaowen, S. Weiwei, L. Leipeng, Z. Mingyang, L. Honghong, B. Lu, Y. Dundong, J. H. Horton, X. Qian and W. Jun, *Applied Catalysis B: Environment and Energy*, 2021, DOI: 10.1016/j.apcatb.2021.120535.
6. G. Sunil More, D. Rajendra Kanchan, A. Banerjee and R. Srivastava, *Chemical Engineering Journal*, 2023, DOI: 10.1016/j.cej.2023.142110.
7. X.-Z. Wei, H. Wang, J. Liu and L. Ma, *Inorganic Chemistry Communications*, 2023, DOI: 10.1016/j.inoche.2023.110956.
8. M. Qiao, J. Ran, T. Yang, Z. Liu and K. Yao, *Catal. Today*, 2024, **437**, NO. 114778.
9. C. Chen, X. Ji, Y. Xiong and J. Jiang, *Green Chemistry*, 2023, DOI: 10.1039/d3gc04067d.
10. Y. Xue, H. Xia, J. Li, J. Su, F. Ge, X. Yang, J. Jiang and M. Zhou, *Chemical Engineering Journal*, 2023, DOI: 10.1016/j.cej.2023.147456.
11. J. Gao, Y. Cao, G. Luo, J. Fan, J. H. Clark and S. Zhang, *Chemical Engineering Journal*, 2022, DOI: 10.1016/j.cej.2022.137723.
12. C. Chen, W. Chen, M. Zhou, Y. Xiong, X. Ji, M. Zhou, L. Zhang, X. Rao and J. Jiang, *Chemical Engineering Journal*, 2024, DOI: 10.1016/j.cej.2024.152353.
13. A. Kumar, R. Bal and R. Srivastava, *ChemCatChem*, 2024, DOI: 10.1002/cctc.202301636.